



## COB-2021-1551

# CHARACTERIZATION OF THE MECHANICAL PROPERTIES OF DIFFERENT METALLIC MATERIALS THROUGH SMALL PUNCH TEST

**Natalia Cordeiro Noce**

**Tatiane de Campos Chuvas**

**Luís Felipe Guimarães de Souza**

**Matheus Campolina Mendes**

Centro Federal de Educação Tecnológica Celso Suckow da Fonseca – CEFET/RJ

natalia.noce@gmail.com tatiane.chuvas@cefet-rj.br lfgs59@gmail.com campolinamendes@gmail.com

**Abstract.** *The small punch test (SPT) is a miniature test firstly developed as a solution for the nuclear industry to evaluate the mechanical properties degradation of industrial components as a non-destructive test. The reduced size specimens (8mm diameter and 0.5mm thick) allow obtaining samples during the industrial component lifespan, without a heavy machining requirement, as mentioned like a non-destructive test. Despite the good accuracy between the results of the mechanical properties of the SPT and the conventional tensile tests, it is still necessary to study the influence of the test parameters on the SPT results due a lack of literature information. In this context, different speed tests were applied on SPT to evaluate how this parameter influences the test results, these, in turn, were also compared with conventional tensile tests. In this work, the SPT results showed a similar behavior to the conventional tensile tests. Analogously, the speed test on SPT must be considered as an important factor to determine the mechanical properties and, also, showed a similar pattern to the conventional tensile tests. On other hand, the small material volume on SPT samples can be a limiting factor for plastic deformation-induced phase transformation sensible materials.*

**Keywords:** *Small Punch Test, Tensile Test, Mechanical Properties*

## 1. INTRODUCTION

Assessment methods for the useful life of equipment are generally conservative, mainly for safety reasons and also because of the uncertainties arising from the lack of data about mechanical properties of specific components, as these properties are modified due to manufacturing processes and technologies applied to produce these parts. Accurately determining the mechanical properties of the material in operation is a key element for improving the reliability of these elements, for optimizing operating procedures, for fixing inspection intervals, and for defining a routine for strategies maintenance and repair, aiming to extend the useful life of the machinery in question (Fleury and Ha, 1998).

Tensile test is the most used to characterize the mechanical properties of materials, since through this test it is possible to obtain the main mechanical properties. In the manufacture of specimens for conventional tensile tests, a relatively large volume of material is required and, furthermore, the tests are usually only completed when the sample breaks, rendering it useless. Consequently, conventional tensile tests are considered destructive (Callister and Rethwisch, 2014).

For this reason, when wanting to evaluate a component inflicting as little damage as possible, it is convenient to use miniature tests such as the Small Punch Test (SPT), which has been developed in order to use a very small volume of material and which can be extracted from the components during their normal useful life, being considered a non-destructive test (Rodríguez *et al.*, 2009).

This work analyzes the mechanical properties of ASTM A335 P92 and AISI 304 steels, through Small Punch Tests and the correlation between the data obtained with those of conventional tensile tests. For this, a device for miniature tests was used, previously designed and manufactured. Complementarily, the best test parameters were studied, such as the displacement speed of the punch.

The results showed that the Small Punch Test described qualitatively well the mechanical behavior of the materials studied, making it possible to formulate equations that correlate the results obtained with those of ultimate tensile strength, yield strength and elongation with those of conventional tensile tests. However, the class of material used is of great importance in the quantitative determination of mechanical properties.

## 2. SMALL PUNCH TEST

The first literature of an assay technique with samples with disk geometry the same size as a specimen for transmission electronic microscopy (TEM) was presented by Manahan *et al.* (1981). The test then called Miniaturized Disc Bend Test (MDBT) was developed to evaluate the mechanical properties of components in the nuclear industry and

to verify the action of different levels of radiation in the degradation of equipment. The MDBT was able to determine the biaxial stress/force response, biaxial ductility, stress relaxation behavior, biaxial creep response and biaxial creep ductility. For the tests, samples with dimensions of 3.0 mm in diameter and 0.25 mm in thickness were used. The tests were performed in a conventional tensile machine using an adaptation, which consists of a device for fitting the disc with a punch for uniaxial compression of the specimen (Figure 1a). From this test it is possible to obtain a curve of punch displacement vs. applied load. With this research, some important information was also obtained, such as the influence of temperature on the test, the influence of the punch tip diameter and its displacement rate for more accurate results.

Nowadays, the test has been called the Small Punch Test and is being studied as an alternative to conventional tests for the analysis of mechanical properties and creep resistance. The European Committee for Standardization (CEN) created document CWA 15627:2006 which presents a set of practice standards for carrying out the SPT, aiming to produce an industry pattern and test methodology. The code of practice sets out recommendations for testing parameters, analysis of data obtained by it and possible geometries for specimens. CWA 15627:2006 foresees a specimen with a diameter (D) of 8.0 mm and a thickness ( $t_0$ ) of 0.5 mm, but square specimens and thickness variations between 0.2 and 0.6 mm can also be used. Since its creation, the technique has been extensively studied in order to find parameters that relate the data obtained with conventional tensile tests.

Figure 1b shows a typical load vs. punch displacement curve to a ductile metal alloy showing the different regions of deformation. The first region (I) corresponds to the elastic flexion of the sample, where it undergoes elastic deformation along with the surface indentation by contact with the punch. Region II describes the progression of plastic deformation through the entire sample, going from the center of the specimen, increasing in the thickness direction and in the radial direction. From a certain point on, the plastic deformation changes to a membrane behavior that occurs due to the slipping of the layers of the specimen and predominates for most of the test, corresponding to region III. Approaching the maximum load, the slope of the curve begins to decrease, as the failure mechanisms (on a microscopic scale) begin to develop giving rise to the fourth region (IV), where the stretch is then a rupture are produced until the total failure of the sample (García *et al.*, 2014).

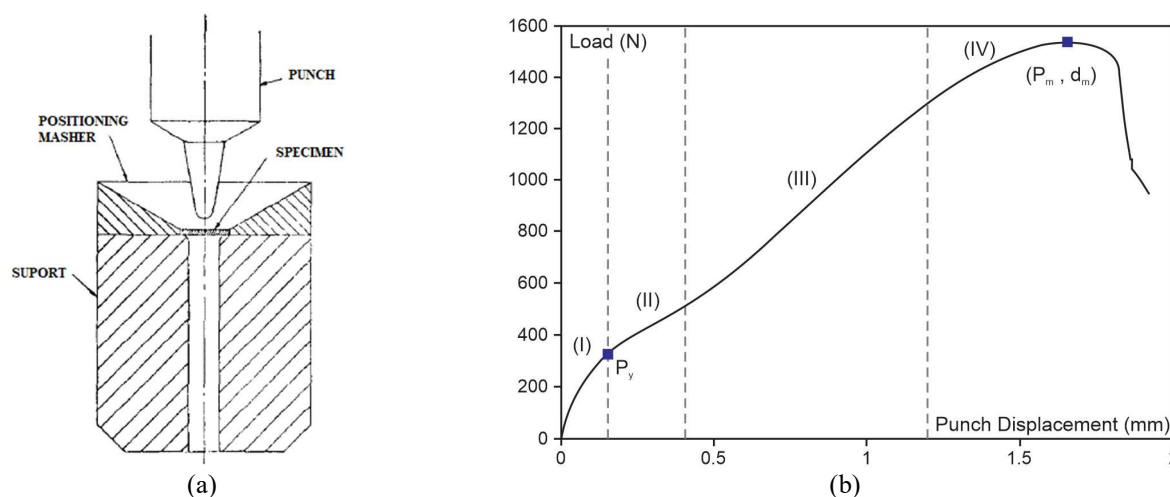


Figure 1. (a) Schematic of Miniaturized Disk Bend Test showing simply supported central loading (Manahan *et al.*, 1981), (b) SPT load vs. punch displacement curve with identification of the different curve zones (García *et al.*, 2014).

Some points of great importance for obtaining the mechanical properties by the SPT are also represented in Figure 1b,  $P_y$  is the load where plastic deformation begins,  $P_m$  is the maximum load obtained during the test and  $d_m$  is the value of punch displacement relative to the fracture point of the sample.

With the use of some empirical and analytical correlations it is possible to establish a correspondence between the results obtained by conventional tensile testing and those obtained by the Small Punch Test and thus acquire some of the mechanical properties of the materials analyzed. García *et al.* (2014) briefly present five methods for the determination of  $P_y$  (Figure 2), data used in the correlation with the yield strength ( $\sigma_{ys}$ ), based on previous research.

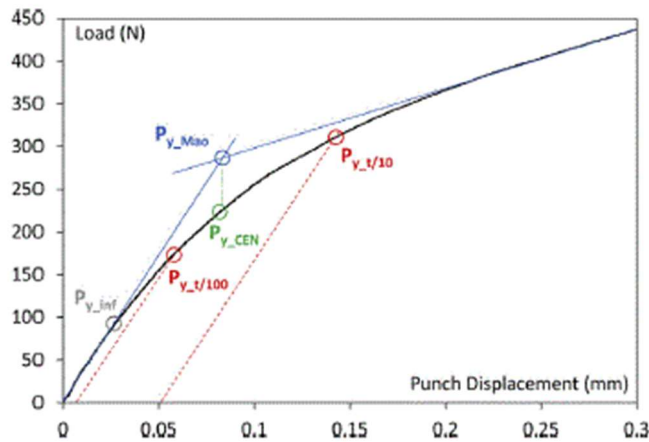


Figure 2. Different proposals for determining  $P_y$  (García *et al.*, 2014).

Mao and Takahashi (1987) define  $P_y$  as the crossing point of two tangents defined in the elastic regime (Region I) and the plastic regime (Region II), called  $P_{y\_Mao}$ . The CEN code of practice contains a slight modification in relation to the one proposed by Mao and Takahashi (1987), it defines  $P_y$  as the vertical projection of the intersection point between two tangents defined between Regions I and II ( $P_{y\_CEN}$ ). Authors such as Contreras *et al.* (2008) and Rodríguez *et al.* (2009) define the load  $P_y$  as the point of intersection between the SPT curve and a straight line parallel to the slope of the graph, with an offset of  $t/10$  or  $t/100$  ( $P_{y\_t/10}$  and  $P_{y\_t/100}$ , respectively), where  $t$  is the thickness of the specimen used in the test. More recently Lacalle *et al.* (2009) have proposed that the load  $P_y$  corresponds to the first inflection point located in region I ( $P_{y\_inf}$ ).

Despite the different ways of determining the load  $P_y$ , there is an agreement among researchers regarding its correlation with the yield strength ( $\sigma_{ys}$ ). The equation is a linear relation (Eq. 1) and depends on the initial sample thickness, the load  $P_y$  and two test constants ( $\alpha_1$  and  $\alpha_2$ ). The test constants are determined experimentally and depend mainly on the type of material, the dimensions of the specimen and the test parameters.

$$\sigma_{ys} = \alpha_1 * \frac{P_y}{t^2} + \alpha_2 \quad (1)$$

where  $\sigma_{ys}$  is the yield strength,  $t$  is the initial thickness of the sample,  $P_y$  is the load associated with yield stress and  $\alpha_1$ ,  $\alpha_2$  are test constants.

For the value of  $P_m$  all the authors mentioned above describe it as the maximum load observed during the test. As there is a difficulty in determining the fracture point of the specimen, the value of  $d_m$  will be defined as the displacement value where the maximum load occurs. The maximum load is linked to the ultimate tensile strength ( $\sigma_{ut}$ ) and in García *et al.* (2014) two correlations obtained experimentally for the determination of this property are presented. First, Eq. 2 was developed and after more recent research Eq. 3 as an alternative for calculating the ultimate tensile strength based on the thickness of the sample and the displacement value at the point of maximum load.

$$\sigma_{ut} = \beta_1 * \frac{P_m}{t^2} + \beta_2 \quad (2)$$

$$\sigma_{ut} = \beta'_1 * \frac{P_m}{(t*d_m)} + \beta'_2 \quad (3)$$

where  $\sigma_{ut}$  is the ultimate tensile strength,  $t$  is the initial thickness of the specimen,  $P_m$  is the maximum test load,  $d_m$  is the punch displacement at the point of maximum load and  $\beta_1$ ,  $\beta_2$ ,  $\beta'_1$ ,  $\beta'_2$  are test constants.

According to García *et al.* (2016) the parameter  $P_m/(t*d_m)$  provides a better estimate for the ultimate tensile strength when working with ductile materials and according to Fernández *et al.* (2015) the most suitable parameter to estimate the ultimate tensile strength in materials that exhibit brittle behavior is  $P_m/t^2$ .

Two different relationships can be found in the literature for determining the elongation ( $A$ ). Fleury and Ha (1998) obtained a linear relationship, described in Eq. 4, where the elongation of the specimen depends on the punch displacement from the point of maximum load, while Rodríguez *et al.* (2009) propose that this property is not only related to the punch displacement at the moment of maximum load, but also the thickness of the specimen used during the test, presented in Eq. 5.

$$A = \gamma * d_m \quad (4)$$

$$A = \gamma' * \frac{d_m}{t} \quad (5)$$

where A is the elongation (%),  $d_m$  is the punch displacement at the point of maximum load, t is the initial thickness of the specimen and  $\gamma, \gamma'$  are test constants.

The punch displacement rate ( $v$ ) during the tests is one of the parameters defined by the CWA 15627:2006 Part B standard. In Eq. 6 is found an estimate for the displacement taking into account the geometry recommended by CEN. Generally speaking, the speed of the punch (displacement of the punch) is in the range between 0.2 to 2.0 mm/min.

$$v = \frac{\varepsilon_{max}}{1000} \quad (6)$$

where  $v$  is the punch displacement rate (mm/min) and  $\varepsilon_{max}$  is the maximum deformation ( $s^{-1}$ ).

### 3. EXPERIMENTAL PROCEDURE

#### 3.1 Materials

When performing the Small Punch Test (SPT) two different types of steel were used, the specimens were manufactured in ASTM A335 P92 steel and AISI 304 steel. Tables 1 and 2 show the chemical compositions of the materials.

Table 1. Chemical composition of ASTM A335 P92 steel (weight %).

| C    | V    | Mn   | W    | Cr   | Ni   | Mo   |
|------|------|------|------|------|------|------|
| 0.11 | 0.23 | 0.30 | 1.62 | 9.62 | 0.10 | 0.50 |

Table 2. Chemical composition of AISI 304 steel (weight %).

| C    | Mn   | P     | S     | Si   | Ni   | Cr    | N     |
|------|------|-------|-------|------|------|-------|-------|
| 0.04 | 1.56 | 0.025 | 0.025 | 0.55 | 8.45 | 18.00 | 0.022 |

ASTM A335 P92 is a ferritic-martensitic alloy steel. It has excellent resistance to high temperatures and creep behavior up to 600 °C. Its chromium content offers excellent resistance to corrosion and oxidation. Compared to other austenitic steels, ASTM A335 P92 steel has higher heat transfer and lower coefficients of thermal expansion.

AISI 304 is a stainless steel (Cr-Ni), with austenitic microstructure, non-hardening and non-magnetic. Its oxidation resistance goes up to a temperature of 850 °C, however its resistance to intracrystalline corrosion is only guaranteed up to a temperature of 300 °C. It has good cold formability, although it requires greater forming efforts than non-alloyed steels. It is indicated for the manufacture of parts that must resist the attack of a large number of corrosive substances, such as nitric acid, alkaline solutions and saline solutions. Austenitic stainless steels maintain their microstructure from room temperature to their melting point and cannot be hardened by quenching heat treatments. Consequently, these steels are generally cold worked to obtain a higher level of hardness.

The mechanical properties of the materials presented in Table 3 were obtained from information contained in the ASTM A335 P92 and AISI 304 standards and from experimental results of conventional tensile tests, at room temperature (only for ASTM A335 P92 steel).

Table 3. Mechanical properties of the materials.

|   | $\sigma_{ys}$ (MPa) | $\sigma_{ut}$ (MPa) | A (%)   |
|---|---------------------|---------------------|---------|
| ASTM A335 P92 Standard                  | > 440               | > 620               | 20      |
| ASTM A335 P92 Conventional Tensile Test | 485                 | 675                 | 26,3    |
| AISI 304 Standard                       | 205 - 350           | 515 - 770           | 35 - 65 |

#### 3.2 Test System

Experimental tests were carried out using a device test like the one used by Manahan *et al.* (1981), which was developed to be coupled to the testing machine of the Laboratório de Materiais (LAMAT) of CEFET/RJ. This device test was manufactured and it is composed of a lower die, an upper die, case and punch as shown in Figure 3.

The device test was coupled to an Instron Testing Machine model 8801 with a 5kN load cell. The lower die is fitted to the machine's lower actuator and the load is applied with its actuation compressing the SPT die against a fixed plate.

All tests were performed at room temperature and without using any type of lubrication. The specific software was used, which enabled the collection and storage of applied force data (N) and of the punch displacement (mm), applying three different test speeds: 0.2mm/min, 0.4mm/min and 0.6mm/min. For this research, a total of 36 specimens were made, 21 of ASTM A335 P92 steel and 15 of AISI 304 steel. At the end, five samples of each of the materials were tested for each proposed test speed.



Figure 3. Device developed for the execution of SPT.

#### 4. RESULTS AND DISCUSSION

After performing all tests, the data were treated in order to express them in load vs. punch displacement curves. In Figure 4 is the comparison between the curves resulting from five SPT tests with a punch displacement speed of 0.4 mm/min for ASTM A335 P92 steel. It is observed in the Figure 4 a similarity in the aspect of the curves obtained in tests performed with the same punch displacement speed, showing that the Small Punch Test presents an efficient rate of repeatability, it can also be seen that the results obtained are compatible with other authors such as Chica *et al.* (2018), Moreno *et al.* (2016) and García *et al.* (2014) for ductile materials. The little variation in the outline of the curve can be clearly seen, especially in points of greater importance such as  $P_m$  and  $d_m$ .

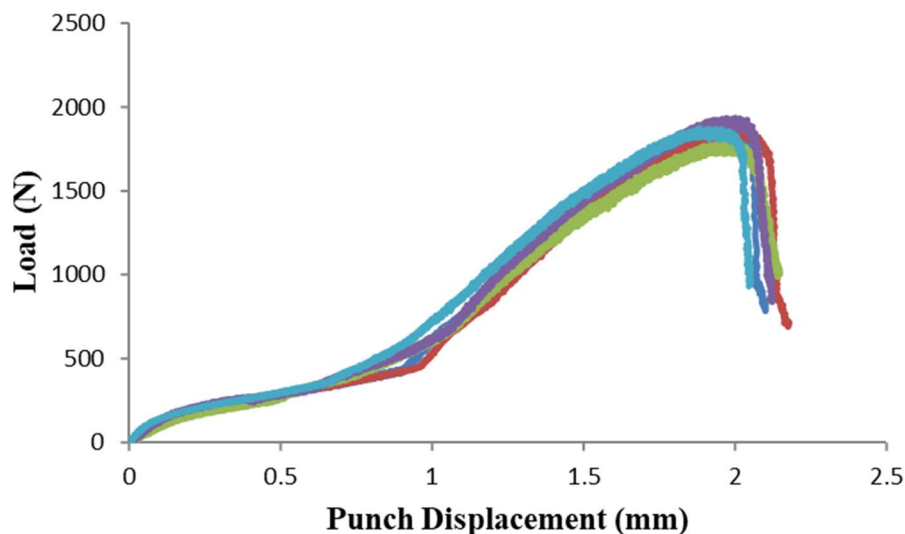


Figure 4. Load vs. punch displacement curves for ASTM A335 P92 steel to SPT with speed of 0.4 mm/min.

The evaluation of the influence of the punch displacement speed is one of the main objectives of this work. Figure 5 shows the comparison between the curves obtained for each material, (a) AISI 304 and (b) ASTM A335 P92, at the three speeds studied. Through the graphics it can be seen that the maximum load value is directly proportional to the speed applied during the test, this behavior is also found during the performance of conventional tensile tests, this is due to an increase in the amount of stacking of dislocations at higher speeds, that is, higher deformation rates causes greater work hardening, thus increasing the maximum load value obtained.

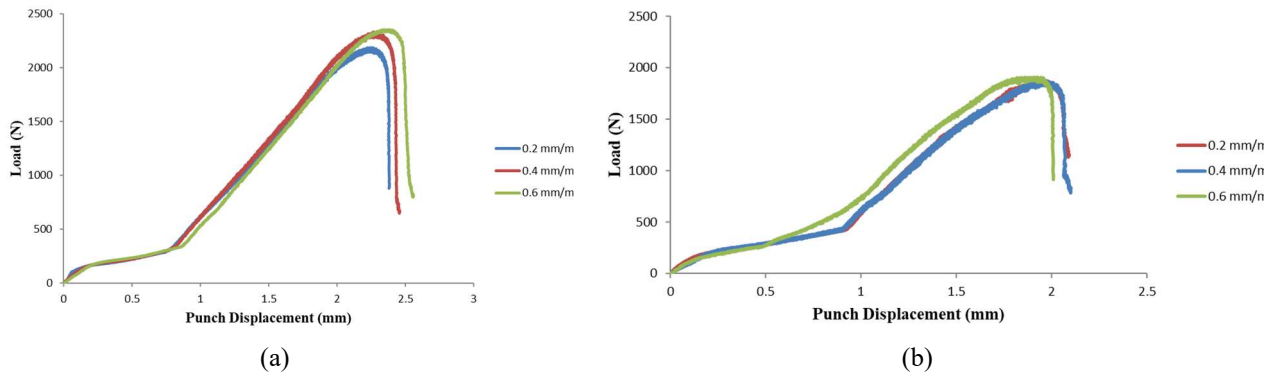


Figure 5. Load vs. punch displacement curves for the different test speeds (a) steel AISI 304 and (b) steel ASTM A335 P92.

#### 4.1 Yield Strength

The yield strength values were determined using the techniques presented by Mao and Takahashi (1987), CEN Code of Practice and Contreras *et al.* (2008). Eq 1 was used, which associates the load  $P_y$ , with the thickness of the specimen and the experimental constants  $\alpha_1$  and  $\alpha_2$ . Employing a graphical method to determine the experimental constants, new constants were developed that were related to the three methods of determining  $P_y$ . The constant  $\alpha_2$  was considered null as a means of simplification presented by García *et al.* (2014).

Using the new calculated test constants, it was possible to obtain the yield strength for each of the tested samples. In Figure 6 shows the average values, as well as the standard deviations, of the results for each material at each test speed used. Values of  $\sigma_{ys}$  in MPa (vertical) and speeds in mm/min.

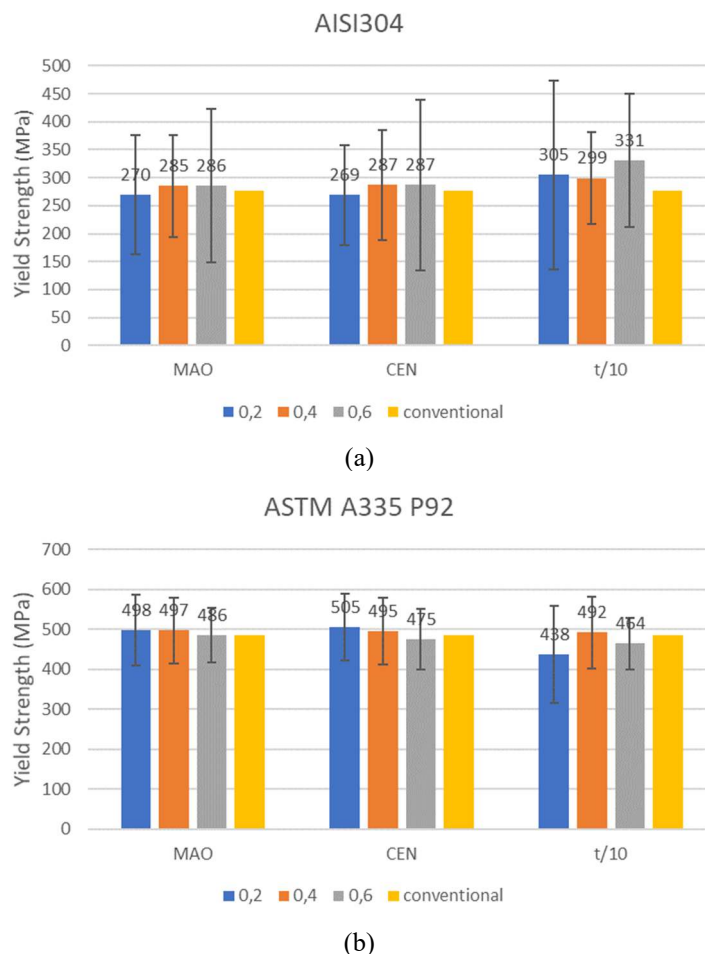


Figure 6. Yield Strength results by SPT for (a) AISI 304 and (b) ASTM A335 P92 steels.

When analyzing Figure 6, it can be seen that for both materials the results for the yield strength are consistent with those of conventional tensile tests for two of the methods for obtaining  $P_y$ , the method presented by Contreras *et al.* (2008) has a significant variation when compared to the other two methods, especially with AISI 304 steel. It was not possible to define a more suitable test speed to be used during the SPT, since the yield strength values do not vary significantly.

#### 4.2 Ultimate Tensile Strength

In determining the ultimate tensile strength, Eq 2 and 3 were used. Equation 2 correlates the maximum load ( $P_m$ ) with the thickness of the specimen ( $t_0$ ) using the experimental constants  $\beta_1$  and  $\beta_2$ . Equation 3 makes use of the displacement of the punch at the point of maximum load ( $d_m$ ), the thickness of the specimen ( $t_0$ ) with the constants  $\beta'_1$  and  $\beta'_2$ . The simplification proposed by García *et al.* (2014) was also used in the determination of the experimental constants for the ultimate tensile strength, so that  $\beta_2$  and  $\beta'_2$  are null.

The same graphic method used to obtain the experimental constants of the yield stress limit was used for the ultimate tensile strength. The results of its application can be seen in Figure 7, and also the standard deviations of the results. Values of  $\sigma_{ut}$  in MPa (vertical) and speeds in mm/min.

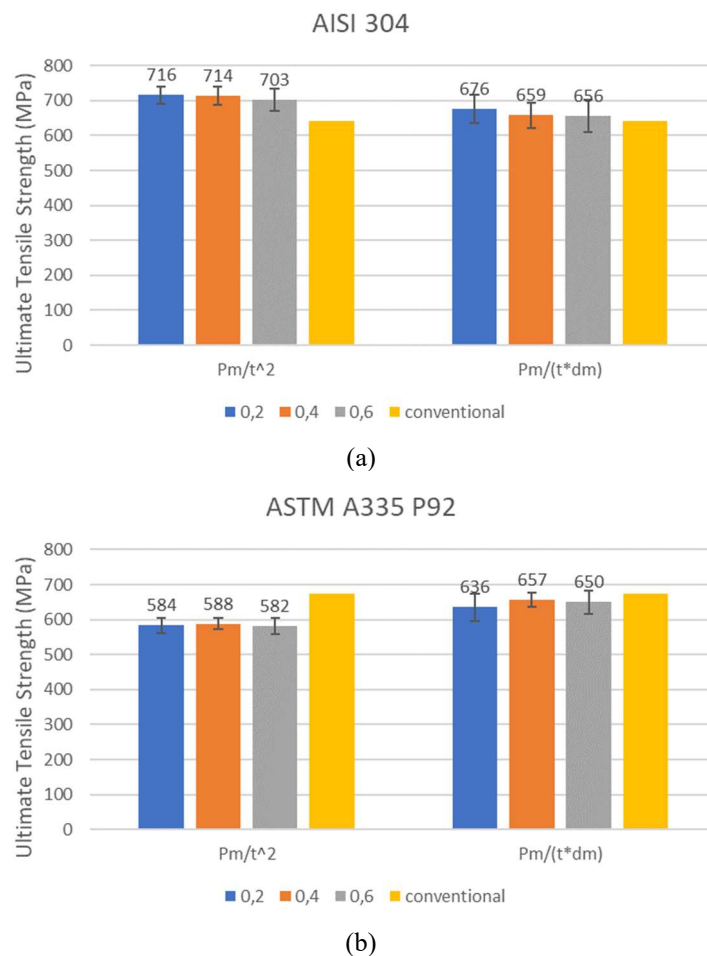


Figure 7. Ultimate tensile strength results by SPT for (a) AISI 304 and (b) ASTM A335 P92 steels.

Analyzing the data obtained in Figure 7, it is observed that the values of the ultimate tensile strength show a range compatible with the results of conventional tensile tests. As previously mentioned for ductile materials, such as those used during the research, Eq 3 would be the most recommended (García *et al.*, 2016) and this can be verified through the results presented.

#### 4.3 Elongation

For the basis for calculating the elongation, Eq 4 and 5 were used, with test constants  $\gamma$  and  $\gamma'$ . Equation 4 relates the constant  $\gamma$  with the displacement at the point of maximum load, and Eq 5 makes use of the constant  $\gamma'$ , the displacement at the point of maximum load and the thickness of the specimen. The same graphical method presented in the previous items was used to determine the values of the experimental constants.

Figure 8 shows the results obtained for the elongation, as the standard deviations. Values of A in percent (vertical) and speeds in mm/min.

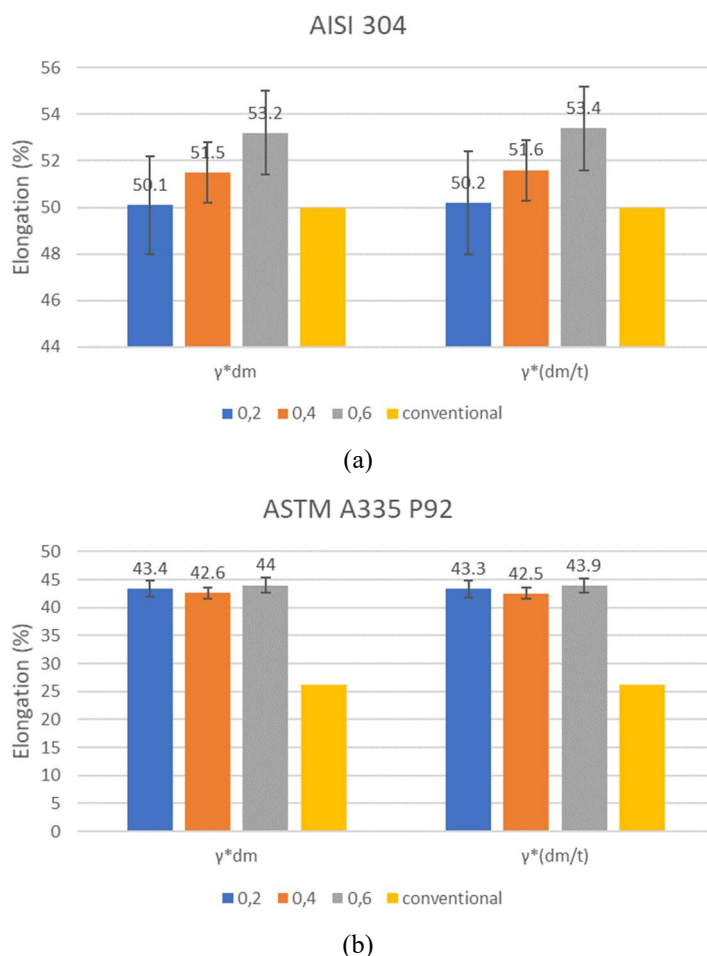


Figure 8. Elongation results by SPT for (a) AISI 304 and (b)ASTM A335 P92 steels.

The results show that the methodology is not efficient for determining the percentage elongation considering that the values are almost double those found in conventional tensile tests, in the case of the ASTM A335 P92 steel. For AISI 304 steel, the results found were closer to those of conventional tensile tests, with a speed of 0.2 mm/min being the most accurate. Due to the similarity between the results found for Eq 4 and 5, it is not possible to determine which one has the best applicability.

#### 4.4 Microstructural Analysis

During the performance of the Small Punch Test, it was observed that in the specimens of AISI 304 steel, when the material made the transition between Region I and Region II, from the elastic deformation phase to the plastic deformation phase, a noise occurred, which resulted in a thickening of the load vs. punch displacement curve. According to Spencer *et al.* (2004) and Costa *et al.* (2016) this noise can be explained by the deformation-induced martensite formation.

To verify if there was some microstructural modification in the stainless-steel specimens, a metallographic examination was performed on samples of the steel, each one corresponding to one of the test speeds used. Figure 9 shows the microstructure of the AISI 304 steel in the as received condition where it is possible to observe its austenitic structure.

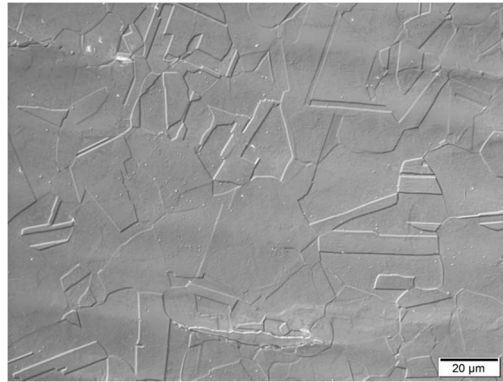


Figure 9. AISI 304 steel microstructure as received.

As can be seen in Figure 10, the specimens present deformation macules with an appearance similar to those found by Bramfitt and Benscoter (2002), which may be an indication of martensite formation. It is possible to infer that the microstructural changes occurring during the SPT test may be impacted the values of the mechanical properties.

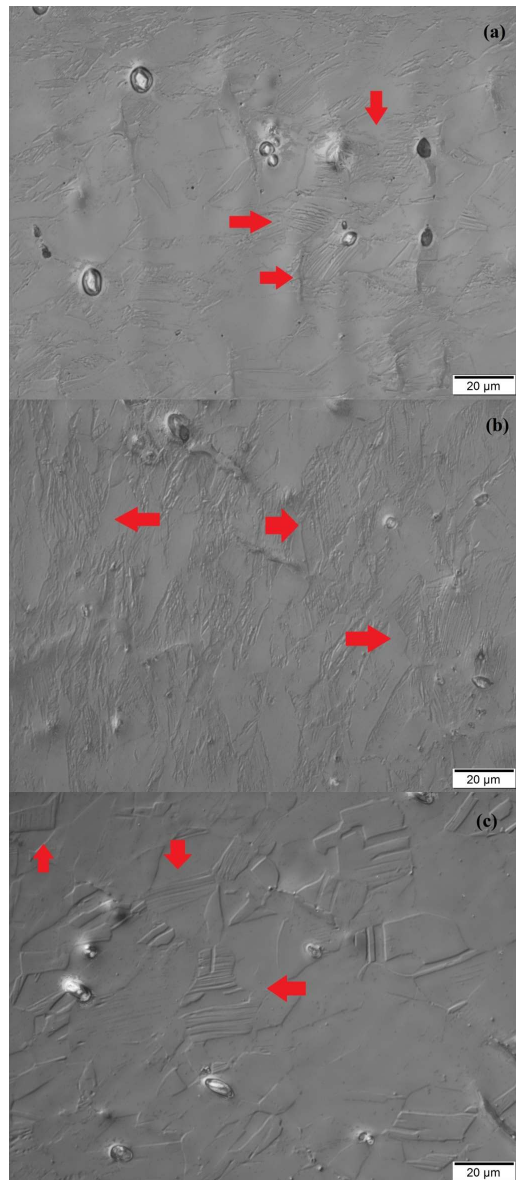


Figure 10. Microscopy of AISI 304 steel for (a) 0.2 mm/min, (b) 0.4 mm/min and (c) 0.6 mm/min. Increase: 1000x.

## 5. CONCLUSIONS

The Small Punched Test is still considered a recent testing technology, so it still must be studied to consolidate the knowledge of the technique. With the evaluation of the results acquired during the performance of this work and the current knowledge about the test, it was concluded that:

1. Load vs. punch displacement curves resulting from the SPT test proved to be qualitatively analogous to conventional tensile tests, also showing good repeatability.
2. For the quantitative determination of mechanical properties, it was evident that it is necessary to separate the materials by class, to obtain results closer to those of conventional tests.
3. It was observed that for materials that may undergo some type of microstructural modification by plastic deformation, such as AISI 304 steel, the Small Punched Test may not reproduce well some of the material's mechanical properties.

## 6. REFERENCES

- Bramfitt, B.L.; Bencotter, A.O., 2002. "Metallographer's Guide Practices and Procedures for Irons and Steels". *ASM International*, 1<sup>st</sup> edition.
- Callister, W.D., Rethwisch, D.G., 2014. "Materials Science and Engineering". *John Wiley & Sons Inc*, 9<sup>th</sup> edition, New York, USA.
- CEN Workshop Agreement, CWA 15627:2006 E, 2006. "Small Punch Test Method for Metallic Materials". *CEN*, Brussels.
- Chica, J.C.; Díez, P.M.B.; Calzada, M.P., 2018. "Development of an improved prediction method for the yield strength of steel alloys in the Small Punch Test". *Material and Design*.
- Contreras, M. A.; Rodríguez, C.; Belzunce, F. J.; Betegón, C, 2008. "Use of small punch test to determine the ductile-to brittle transition temperature of structural steels". *Fatigue & Fracture Engineering Materials & Structures*, v.31, pp. 727-737.
- Costa, D.C.T.; Cardoso, M.C.; Fonseca, G.S.; Moreira, L.P.; Martiny, M.; Mercier, S., 2016. "Strain-induced martensite formation of AISI 304L steel sheet: experiments and modeling". *Materials Science Forum*, v. 869, pp. 490-496.
- Fleury, S.; Ha, J.S., 1998. "Small punch tests to estimate the mechanical properties of steels for steam power plants". *Int. J. Pres.*, vol. 75, pp. 699-706.
- García, T.E.; Rodríguez, C.; Belzunce, F.J.; Cuesta, I.I., 2016. "Effect of hydrogen embrittlement on the tensile properties of CrMoV steels by means of the small punch test". *Materials Science & Engineering A*, v.664, pp. 165-176.
- García, T.E.; Rodríguez, C.; Belzunce, F.J.; Suarez, C., 2014. "Estimation of the mechanical properties of metallic materials by means of the small punched test". *Journal of Alloys and Compounds*, v. 582, pp. 708-717.
- Lacalle, R.; García, J.; Álvares, A. A., 2009. "Obtención mediante el ensayo small punch de las propiedades de tracción de materiales metálicos" *Anales de Mecánica de la Fractura*, vol. 2, pp. 501-506, Santander.
- Manahan, M. P.; Argon, A. S.; Harling, O. K., 1981. "The development of a miniaturized disk bend test for the determination of post-irradiation mechanical properties". *Journal of Nuclear Materials*, v. 104, pp. 1545-1550.
- Mao, X.; Takahashi, H., 1987. "Development of a further-miniaturized specimen of 3 mm diameter for TEM disk ( $\phi$  0,3 mm) Small Punch Test". *Journal of Nuclear Materials*, vol.150, pp. 42-52.
- Moreno, M.F.; Bertolino, G.; Yawny, A., 2016. "The significance of specimen displacement definition on the mechanical properties derived from Small Punch Test". *Material and Design*, v. 95, pp. 623-631.
- Rodríguez, C.; García Cabezas, J.; Cárdenas, E.; Belzunce, F. J.; Betegón, C., 2009. "Mechanical properties characterization of heat-affected zone using the small punch test". *Welding Journal*, v. 88, pp. 188-192.
- Spencer, K.; Embury, J.D.; Conlon, K.T.; Véron, M.; Bréchet, Y., 2004. "Strengthening via the formation of strain-induced martensite in stainless steels". *Materials Science & Engineering A*, v. 387-389, pp. 873-881.

## 7. RESPONSIBILITY NOTICE

The authors are the only responsible for the printed material included in this paper.